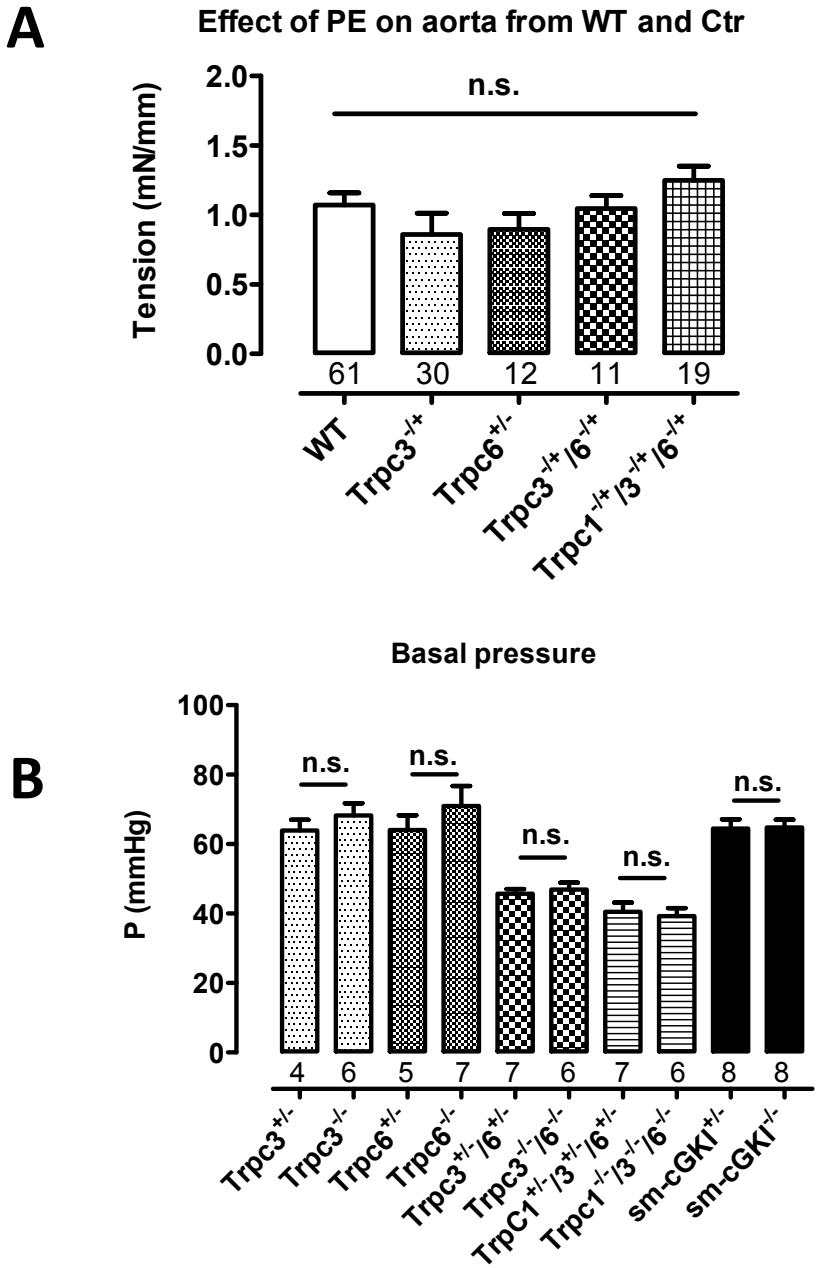

Supplemental Figure 1:

A: Magnitudes of PE-induced contractions in aortic rings from the indicated mouse line with intact endothelium. No difference was found between values from wild type and heterozygous mice. Columns represent mean ± SEM. Numbers represent the number of experiments. Data were analyzed using ANOVA followed by Bonferroni post hoc test. n.s., non-significant

B: Magnitudes of pressure in hind limbs from the indicated mouse lines in control conditions . Columns represent mean ± SEM. Numbers represent the number of experiments. Data were analyzed using Student's t-test. No statistically significant differences was found between heterozygous and the respective knockout mouse strain. n.s., non-significant

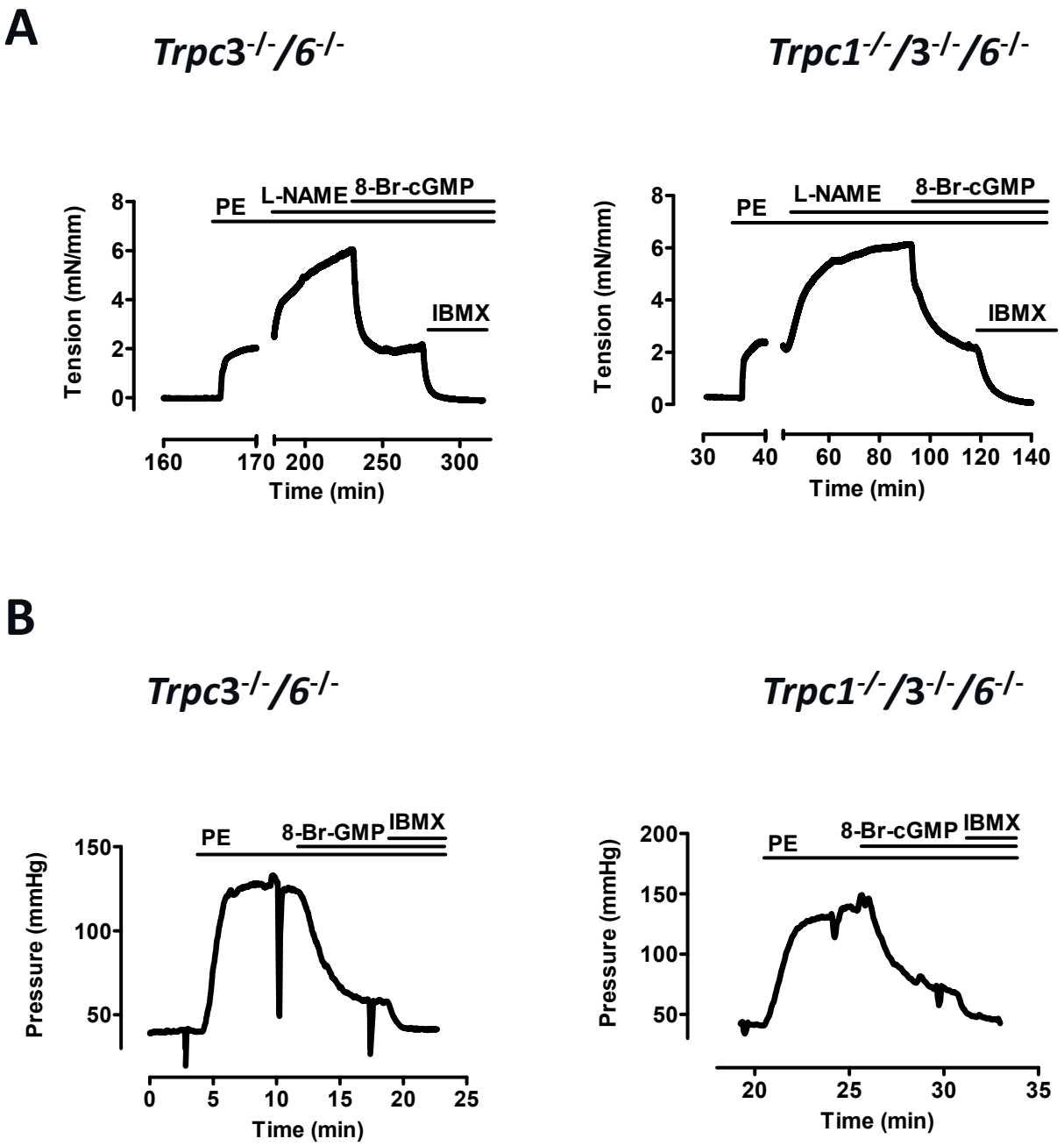

Supplemental Figure 2: Original recordings of PE-induced stimulation in murine aorta (A) and hind limb (B) from a Trpc3$^{-/-}$/6$^{-/-}$ and a Trpc1$^{-/-}$/3$^{-/-}$/6$^{-/-}$ mouse. Bars indicate the presence of PE (3 µM (aorta) or 10 µM (hind limb)), L-NAME (100 µM), 8-Br-cGMP (300 µM), and IBMX (100 µM). Please note that, in A, different time scales were used to make the effect of PE clear.

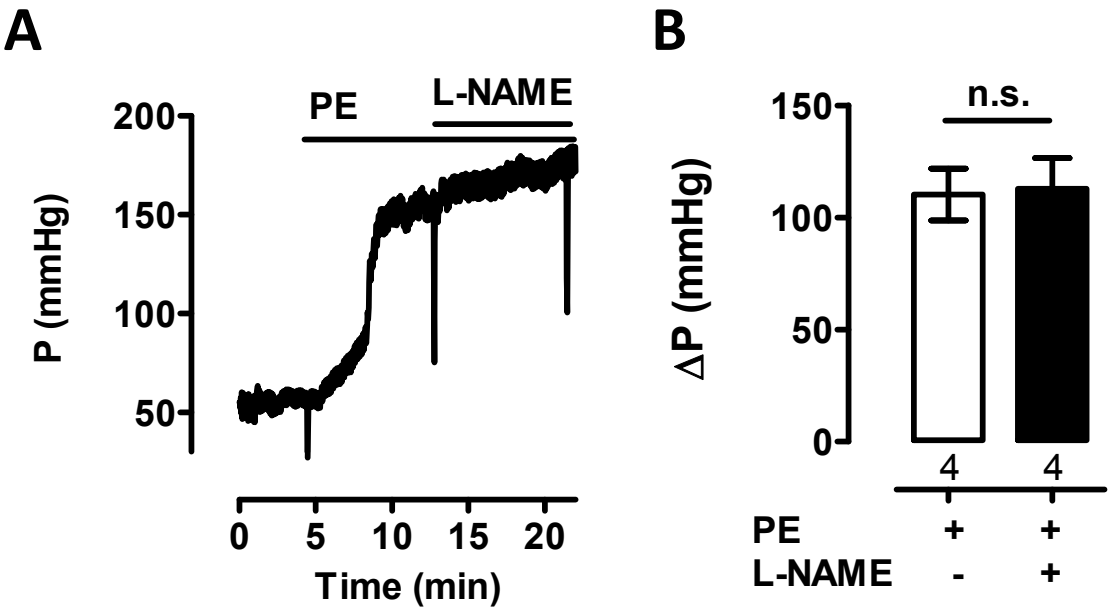

Supplemental Figure 3:
Effect of L-NAME on the magnitude of PE-induced pressure increase in murine hind limb
A: Original recordings of PE-induced pressure increase in hind limb from a WT mouse. Bars indicate the presence of PE (10 µM) and L-NAME (100 µM).
B: Magnitudes of PE-induced pressure increase in the absence and presence of L-NAME. Columns represent mean ± SEM. Numbers represent the number of experiments. Data were analyzed using paired Student's t-test. n.s., non-significant.

Supplemental Figure 4: Magnitudes of PE-induced contractions in intact murine aorta

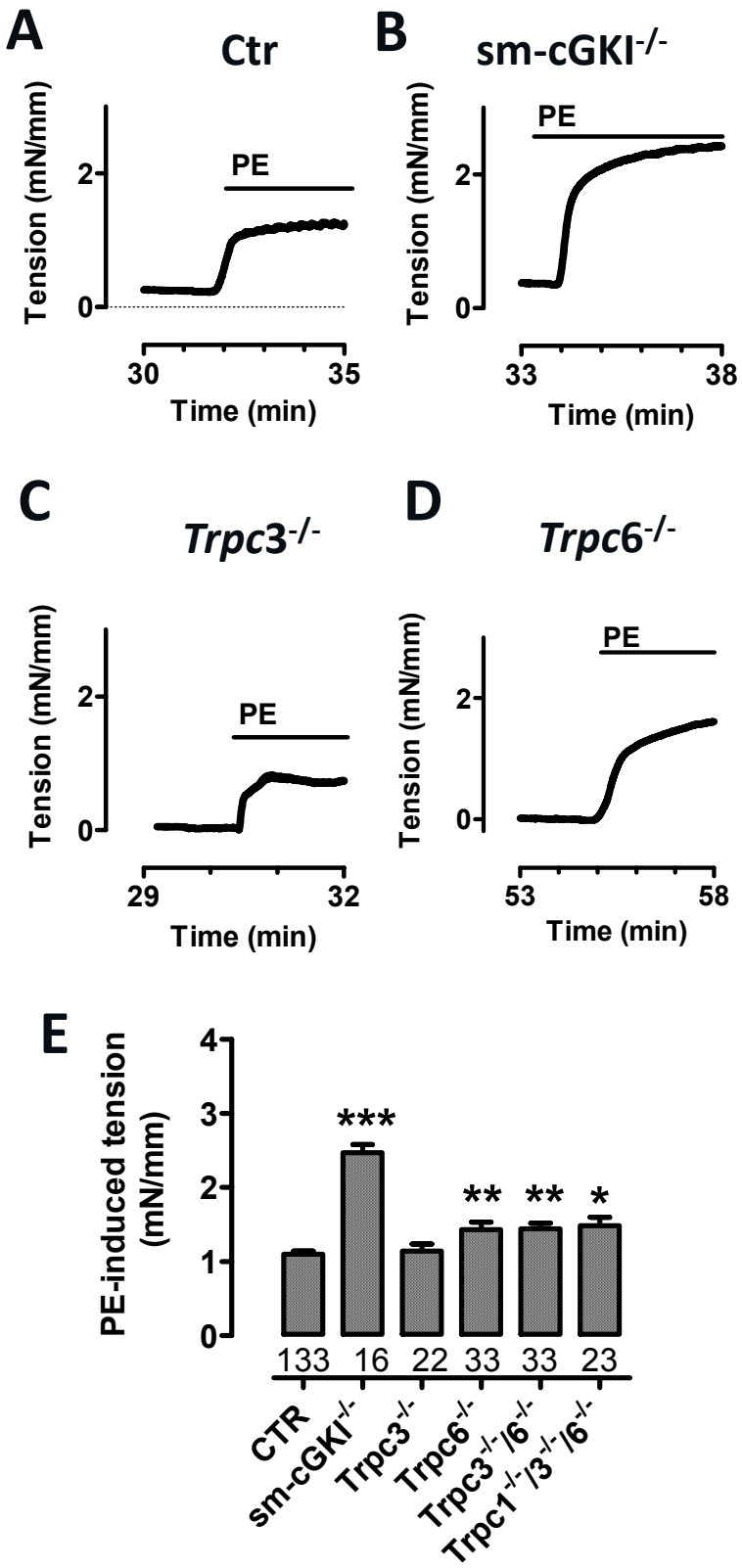

Suppl. Figure 4: Magnitudes of PE-induced contractions in intact murine aorta
A-D: Original recordings of PE-induced contraction in aortic rings from a CTR (A), sm-cGKI$^{-/-}$ (B), *trpc*3$^{-/-}$ (C), and *trpc*6$^{-/-}$ (D) mouse. Bars indicate the presence of PE (3 µM). Please note that the traces are from Fig 1 using an expanded time scale.
E: Magnitudes of PE-induced contractions in aortic rings from the indicated mouse line with intact endothelium. Columns represent mean ± SEM. Numbers represent the number of experiments. Data were analyzed using ANOVA followed by Bonferroni post hoc test. Asterisks indicate a significant difference from Ctr with ***, $p < 0.001$; **, $p < 0.01$; *, $p < 0.05$.

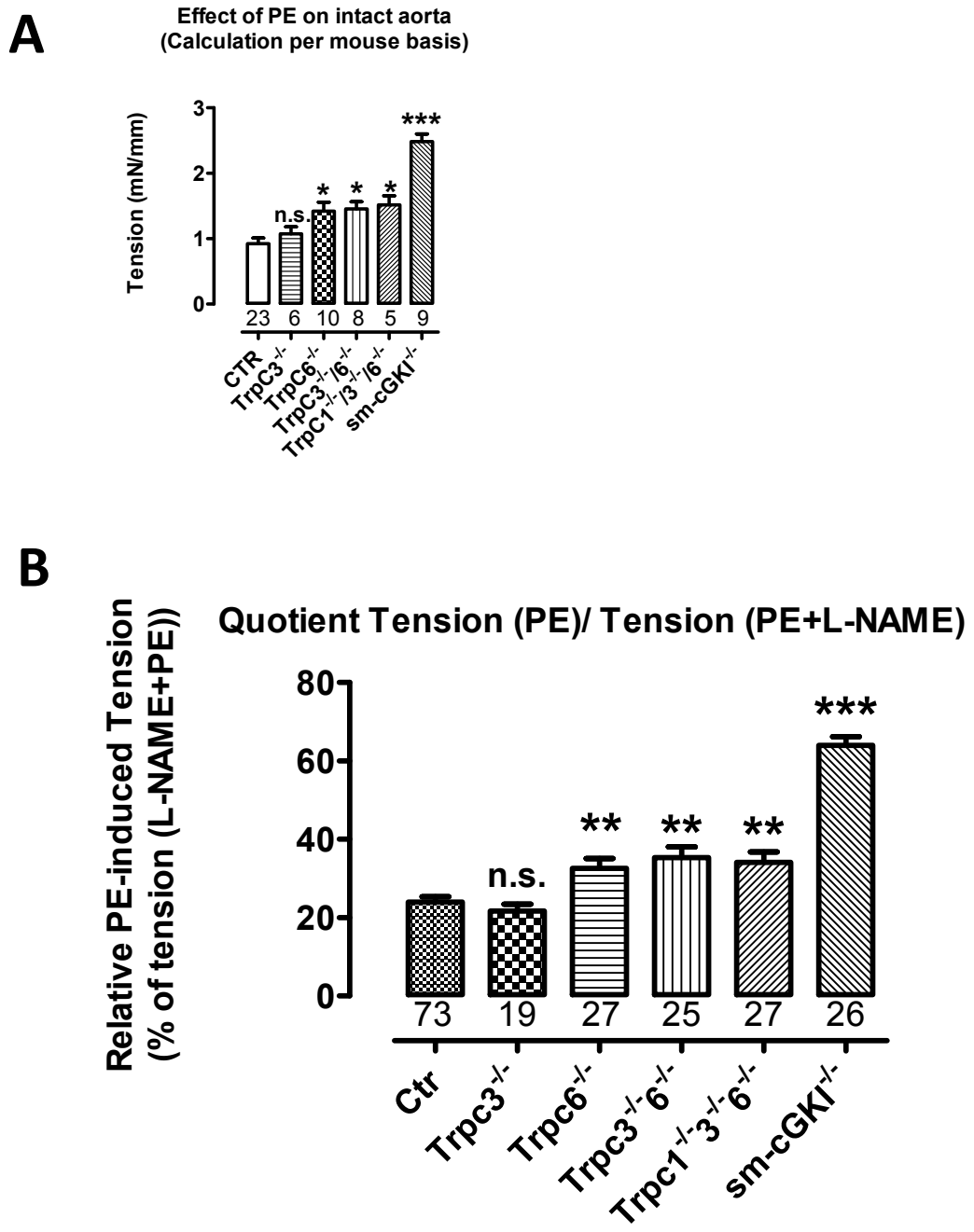

Supplemental Figure 5:
A: Calculation of Suppl. Fig. 3E on per-mouse basis.
B: Relative magnitudes of PE-induced contractions in aortic rings from the indicated mouse line with intact endothelium. Values were calculated as the ratio of the tension induced by PE (3µM) and the tension in the presence of both PE and L-NAME (100 µM). Columns represent mean ± SEM. Numbers represent the number of experiments. Data were analyzed using ANOVA followed by Bonferroni post hoc test. n.s., non-significant; *, $p < 0.5$; **, $p < 0.01$; ***, $p < 0.01$

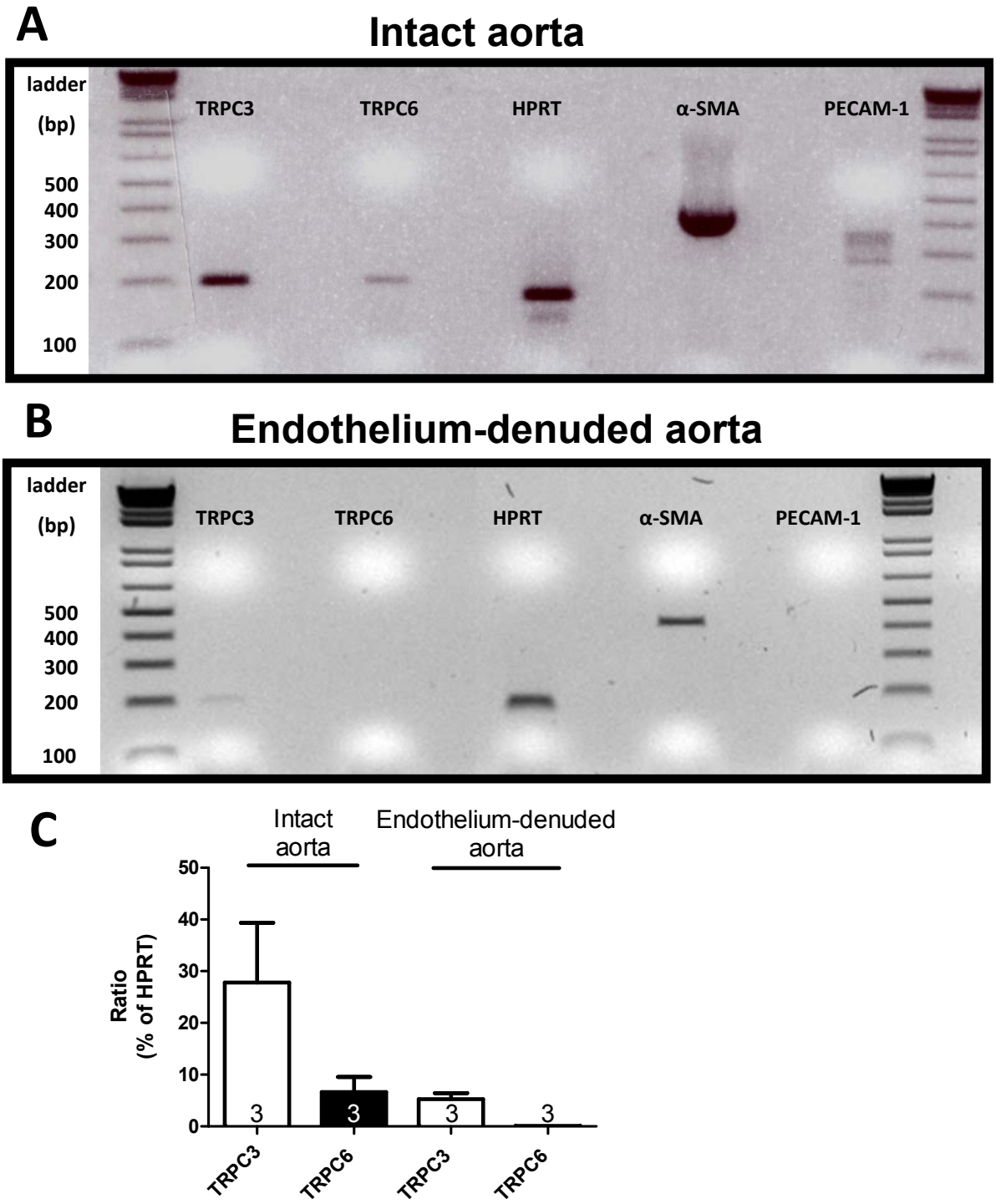

Supplemental Figure 6: Analysis by PCR of total RNA from intact and endothelium-denuded aorta. A, B. Analysis of PCR products by agarose gel electrophoresis in intact aorta (A) and endothelium-denuded aorta (B). C. Quantitative analysis. Amplification products were obtained with primer pairs described in the expanded Methods section. Primer pairs against HPRT, α-SMA, and PECAM-1 were used as references. Amplification products for α-SMA and PECAM-1 were detected in intact aorta whereas only products for α-SMA were detected in endothelium-denuded aorta confirming the absence of endothelium in the latter preparation. Values are calculated as the ratio of the signals for the respective TRPC channel and HPRT and shown as mean ± SEM. Numbers represent the number of experiments.

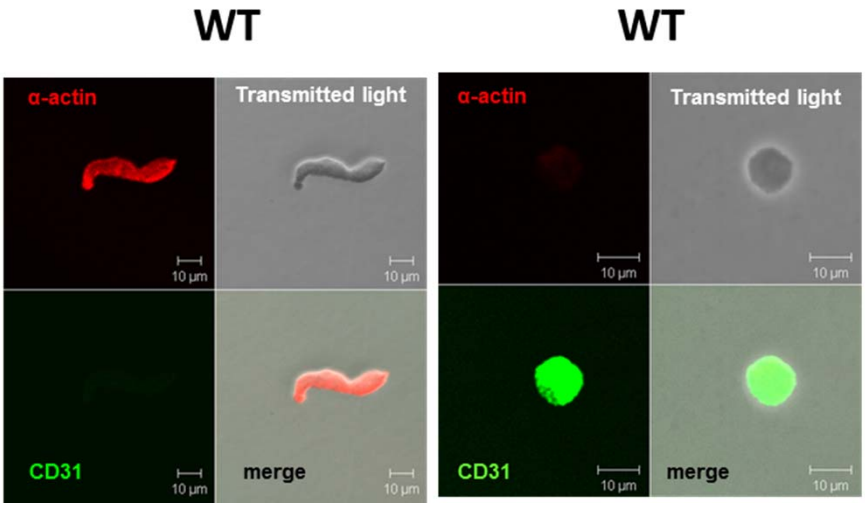

Supplemental Figure 7:
Immunolabelling of isolated VSMC (left) and EC (right) from a wild type (WT) mouse with anti-α-actin and anti-CD31 antibodies Markers for VSMC (α-actin) and for EC (CD31) specifically decorated the respective cells. Identical results were obtained in 3 independent experiments.

Supplemental Figure 8: Expression of TRPC3 and TRPC6 channels and cGKI in smooth muscle cells from murine aorta

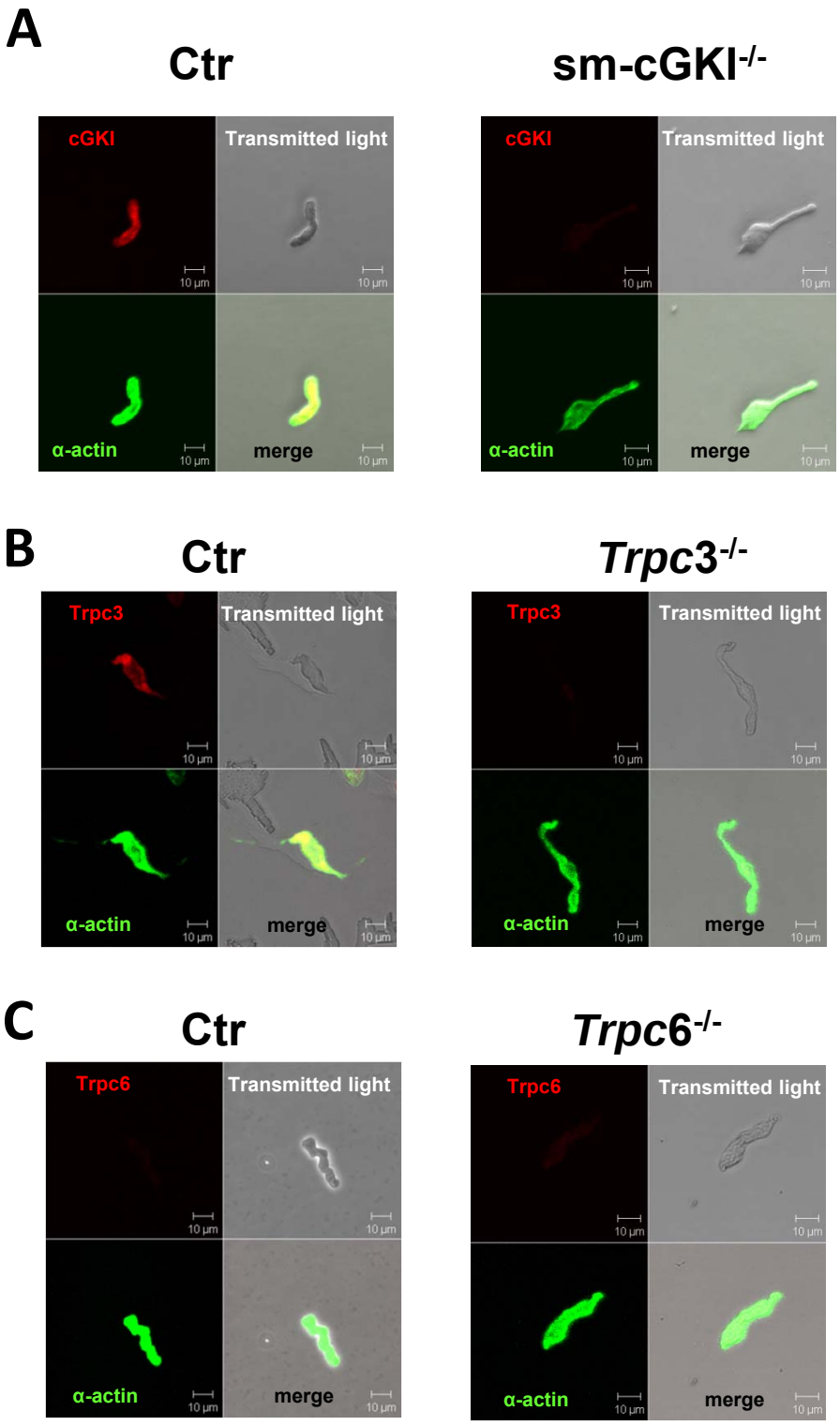

Suppl. Figure 8: Expression of TRPC3 and TRPC6 channels and cGKI in vascular smooth muscle cells (VSMC) from murine aorta
A: Immunolabelling of isolated VSMC from a Ctr (left) and a sm-cGKI$^{-/-}$ (right) mouse with anti-α-actin and anti-cGKI.
B: Immunolabelling of isolated VSMC from a Ctr (left) and a *trpc*3$^{-/-}$ (right) mouse with anti-α-actin and anti-TRPC3.
C: Immunolabelling of isolated VSMC from a Ctr (left) and a *trpc*6$^{-/-}$ (right) mouse with anti-α-actin and anti-TRPC6.
Identical results were obtained in 3 independent experiments from each mouse line (see Suppl. Fig 3).

Supplemental Figure 9A: Immunolabelling of isolated EC

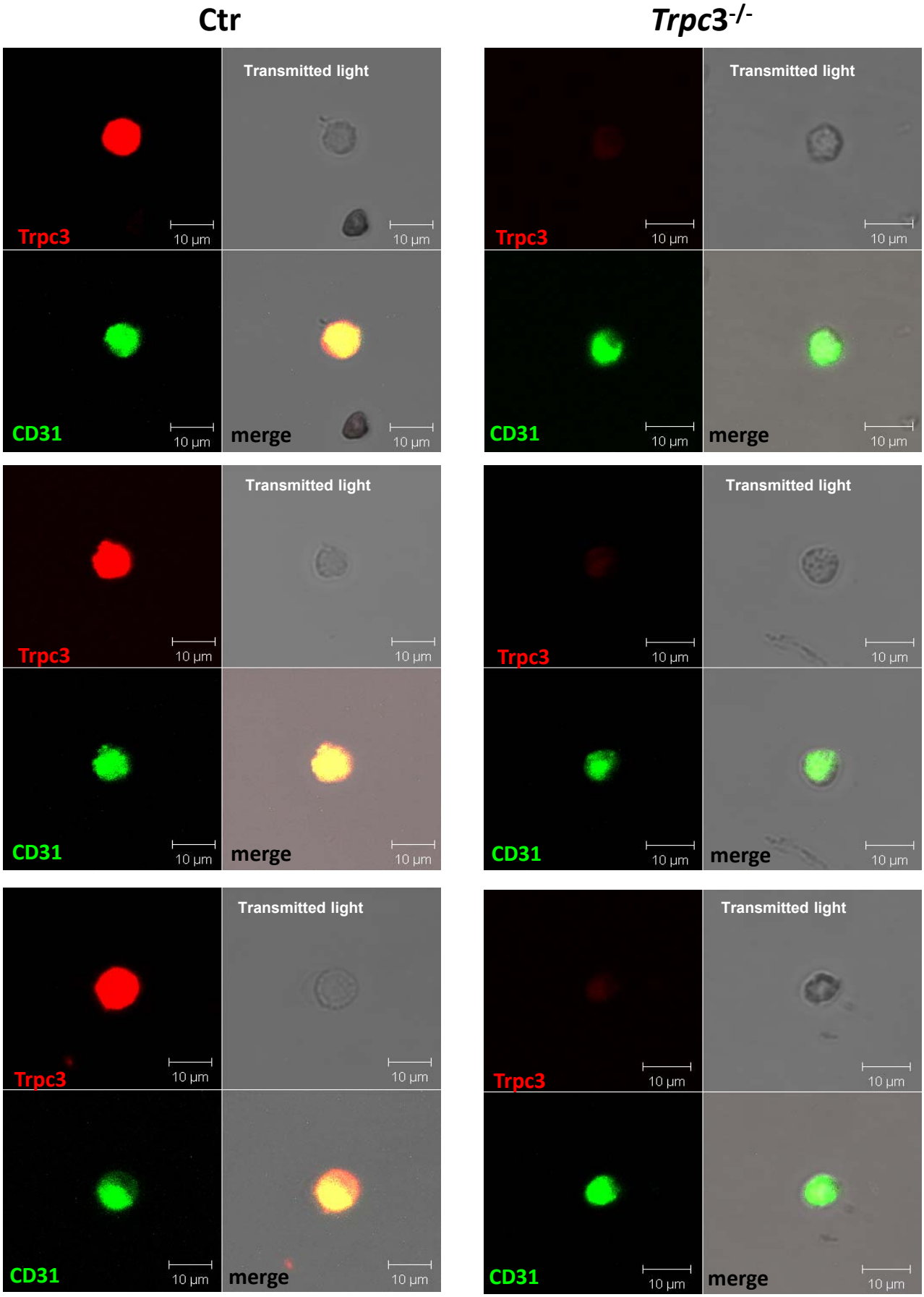

Supplemental Figure 9B: Immunolabelling of isolated EC

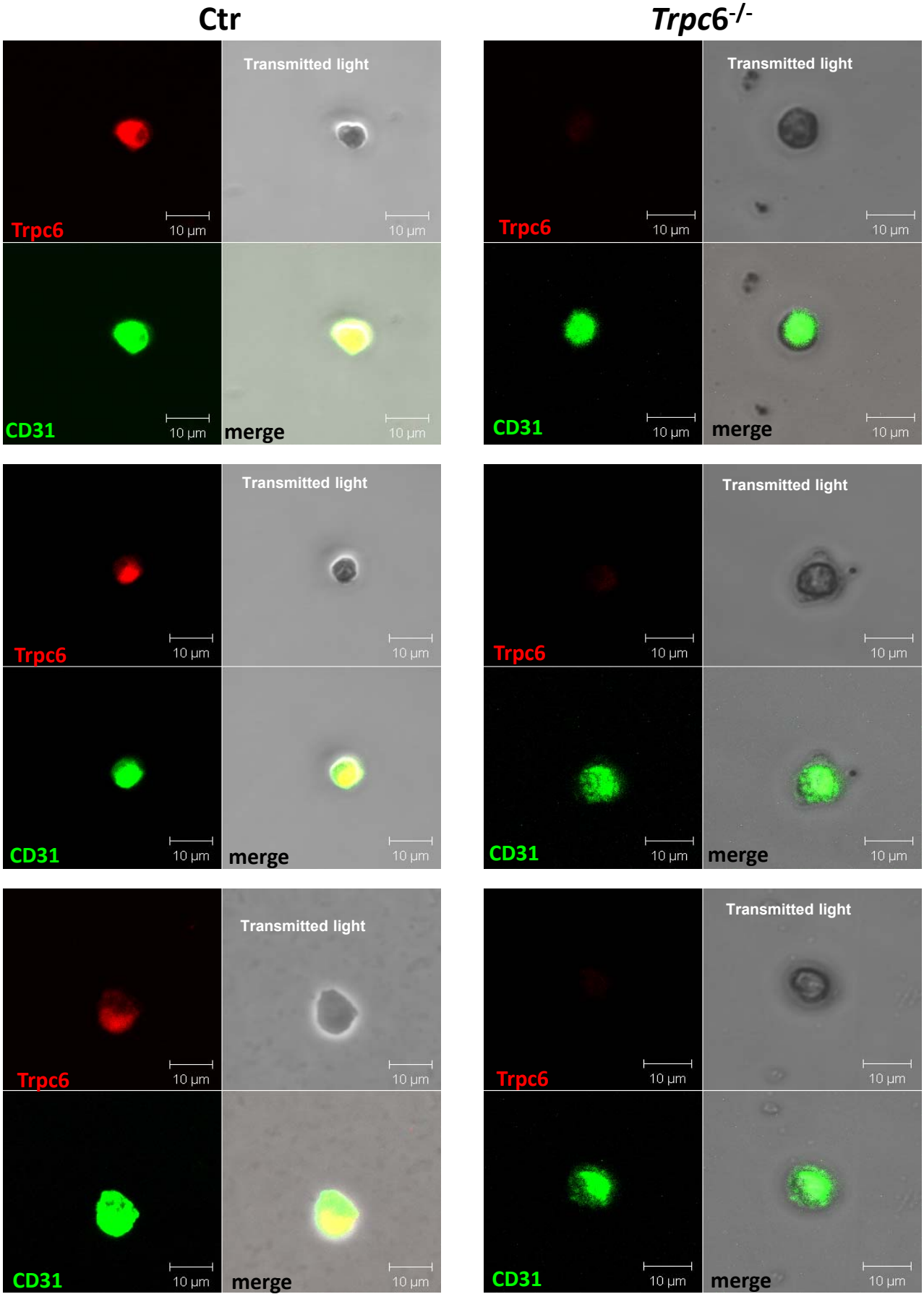

Supplemental Figure 9C: Immunolabelling of isolated SMC

Ctr **sm-cGKI$^{-/-}$**

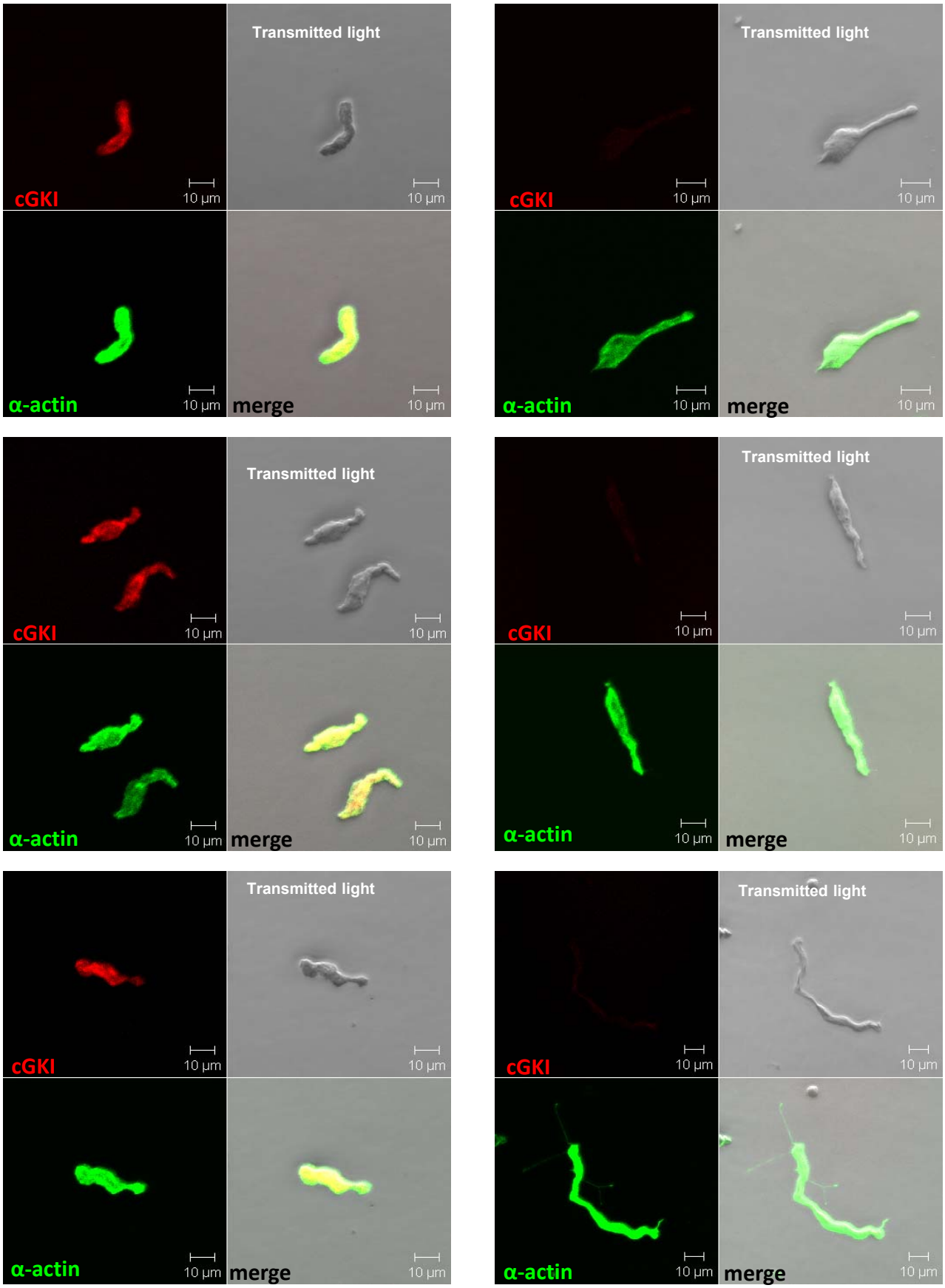

Supplemental Figure 9D: Immunolabelling of isolated SMC

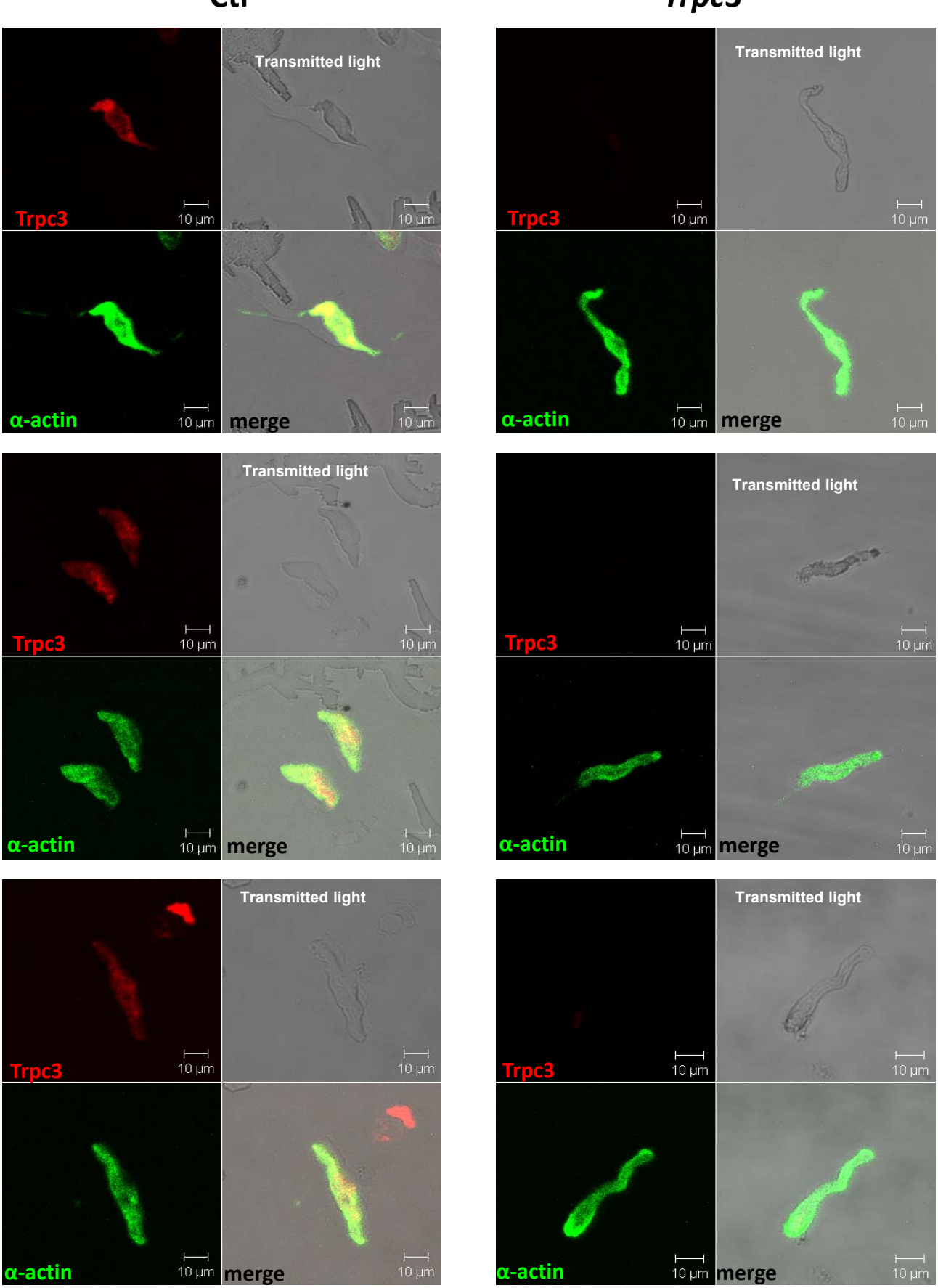

Supplemental Figure 9E: Immunolabelling of isolated SMC

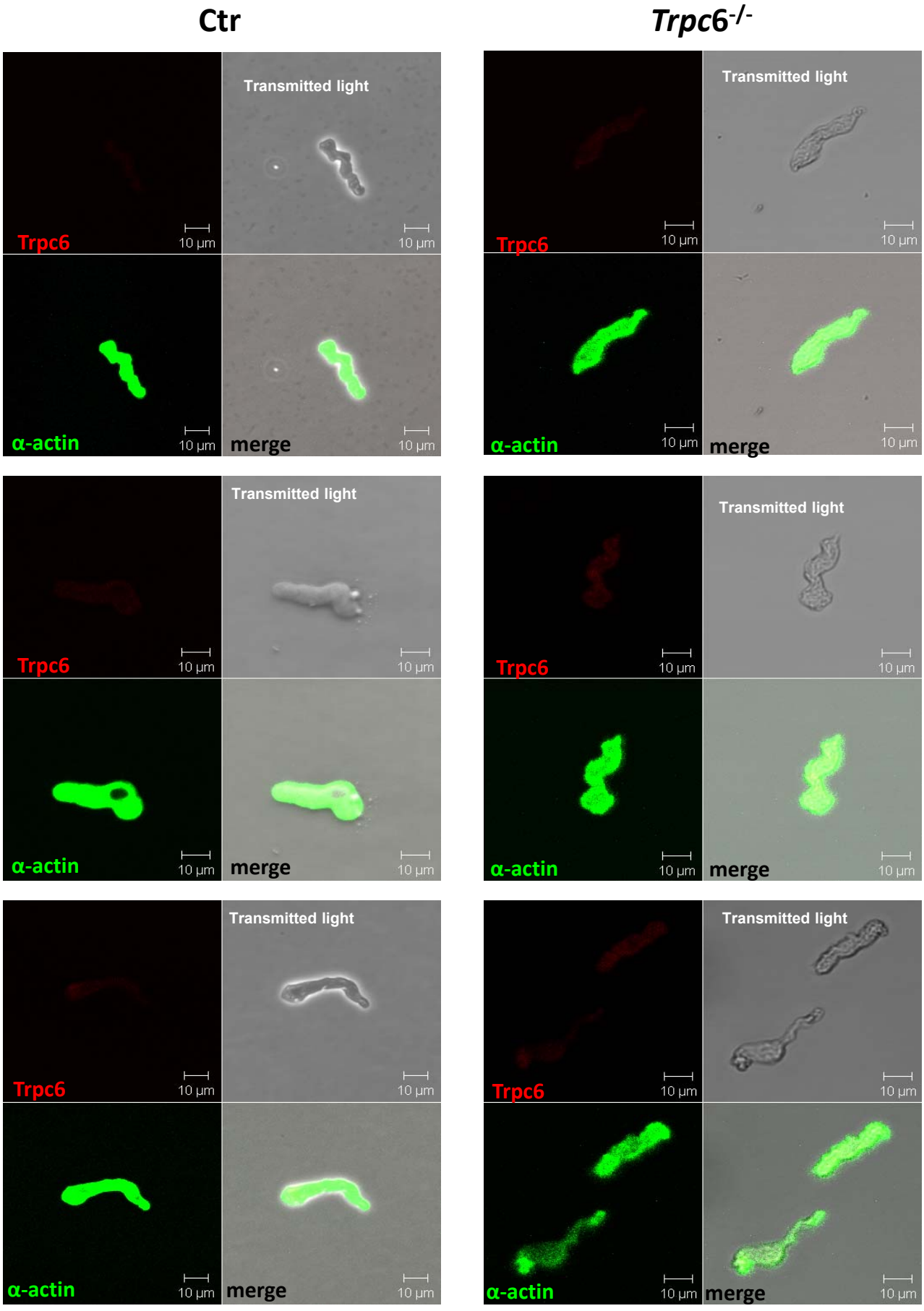

Supplemental Figure 9 A-E:
Immunolabelling of isolated EC and VSMC from a Ctr (left) and from a the indicated mouse model (right) with the indicated antibodies. EC and SMC were isolated from one aorta and decorated differentially with the respective antibodies. Each picture corresponds to a single experiment.

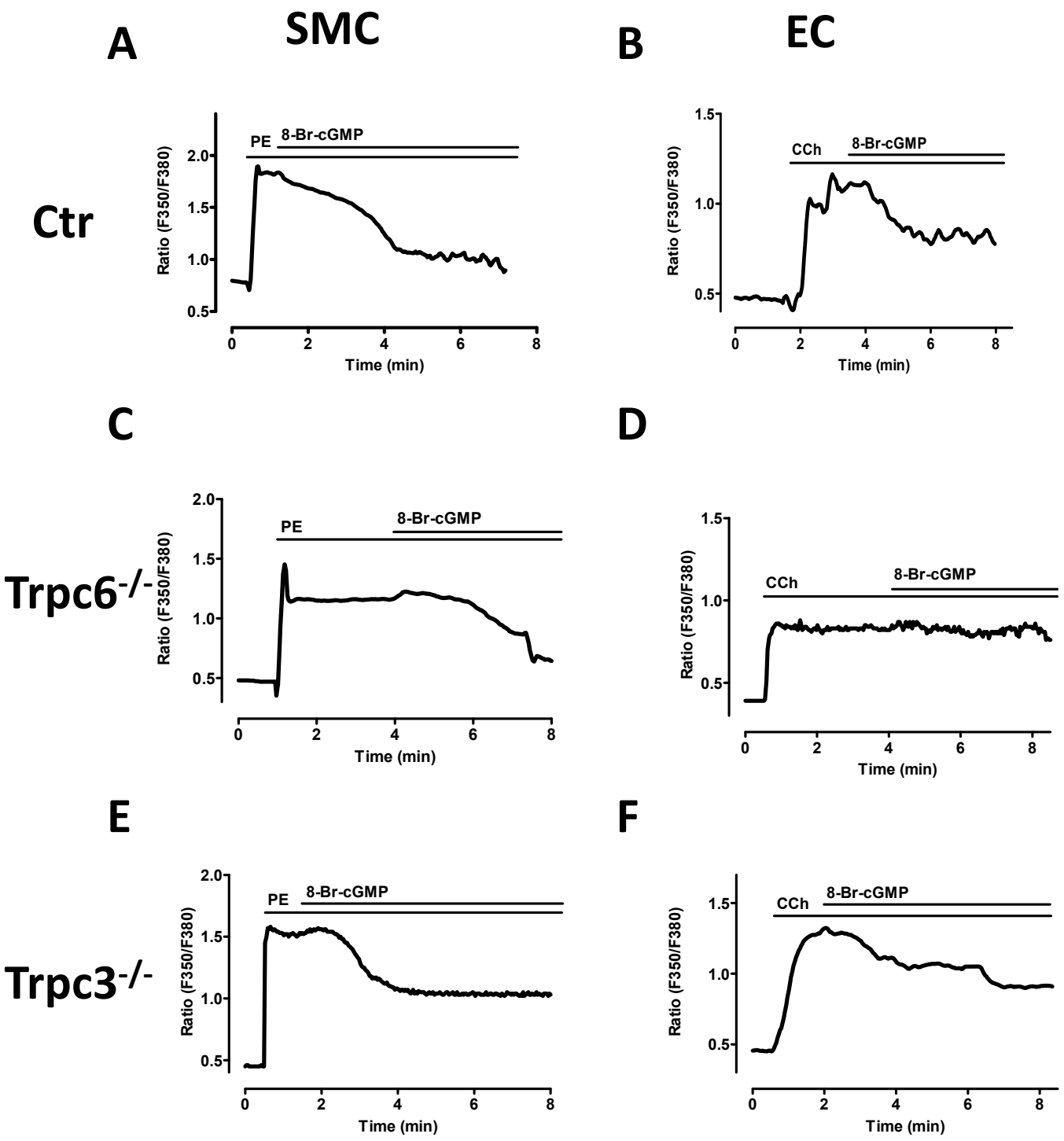

Supplemental Figure 10:
Original recordings of intracellular [Ca^{2+}] in aortic smooth muscle cells (SMC, left) and aortic endothelial cells (EC, right) from a CTR (A, B), $Trpc6^{-/-}$ (C, D), and $Trpc3^{-/-}$ (E, F) mouse. Bars indicate the presence of PE (30 µM), CCh (30 µM), and 8-Br-cGMP (300µM), respectively.

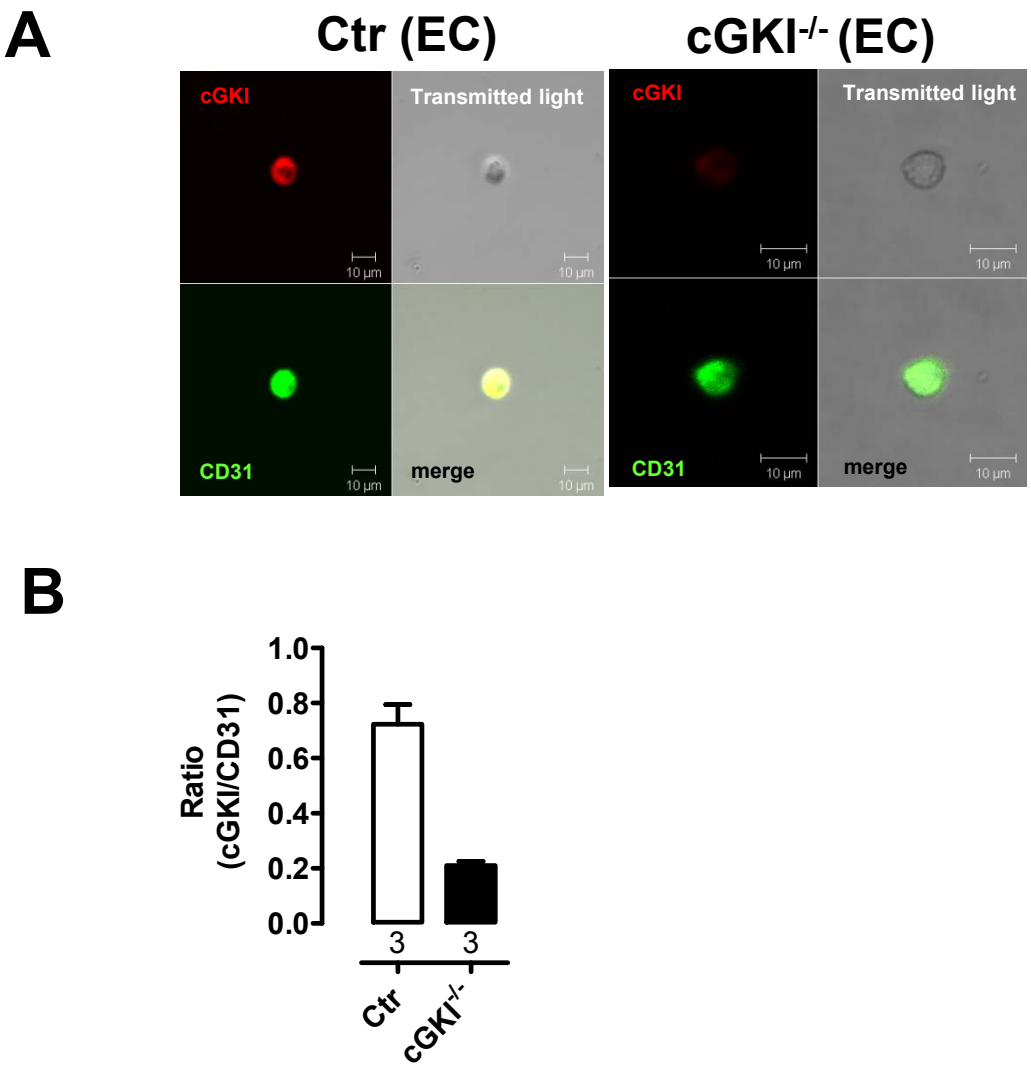

Supplemental Figure 11:
A: Immunolabelling of isolated endothelial cells (EC) from a Ctr (left) and from a cGKI$^{-/-}$ mouse (right) with anti-cGKI and anti-CD31. The cGKI$^{-/-}$ mouse has been described by Pfeifer et al, 1998, EMBO J 17:3045.
B: Signal ratios. Relative Intensities were calculated as the ratio of the signals of anti-cGKI and anti-CD31. Columns represent mean ± SEM. Numbers represent the number of cells.

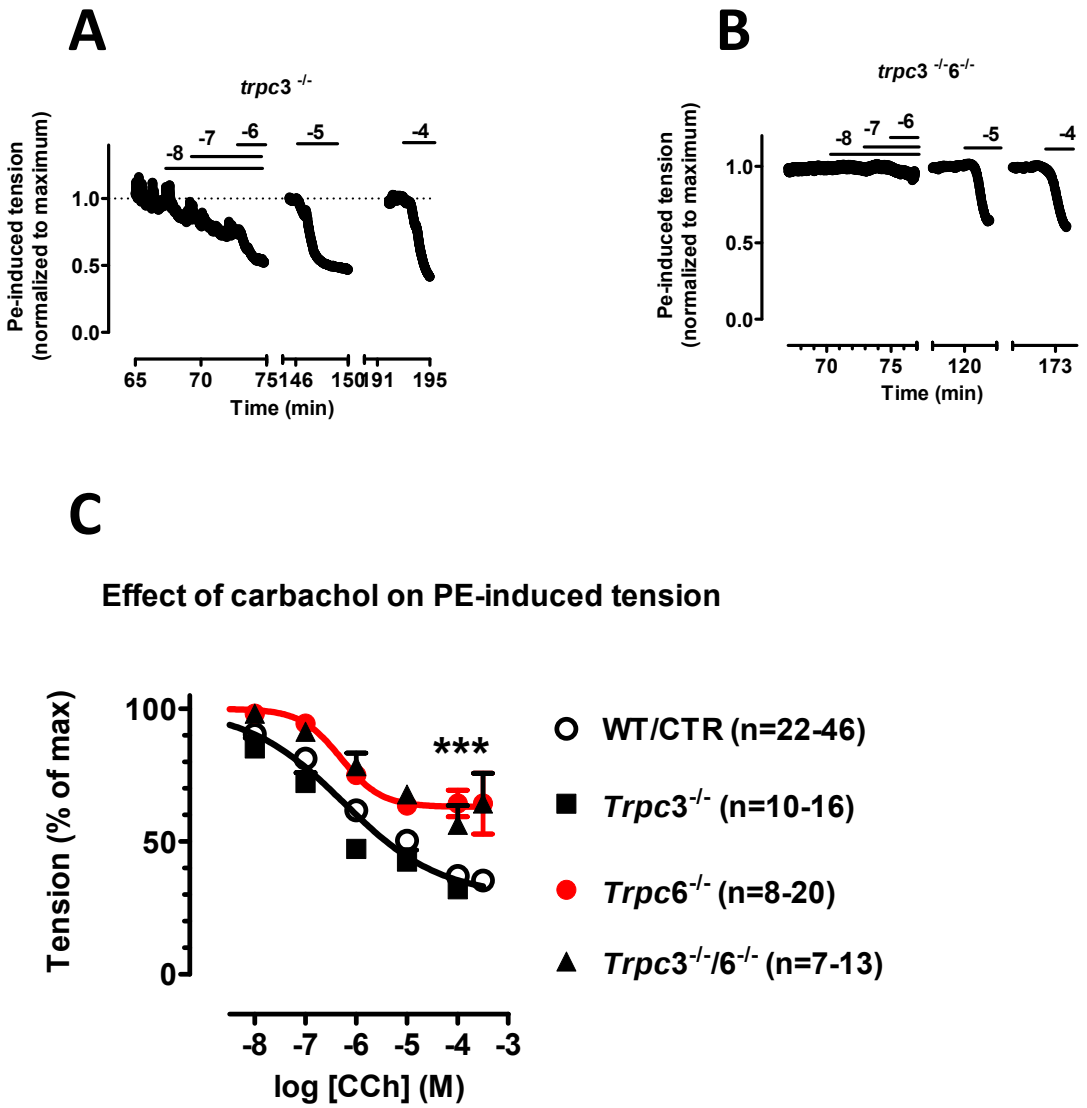

Supplemental Figure 12:

A, B: : Original recordings of CCh-induced relaxations in aortic rings from a trpc3-/- (C), and trpc3-/-6-/- (D) mouse. PE (3 µM) was present throughout the experiment. Bars indicate the presence of CCh in log (M).

C: Concentration-response curves of carbachol on PE (3 µM) - induced contraction of aortic rings from Ctr, *Trpc*3$^{-/-}$, and *Trpc*6$^{-/-}$, and *Trpc*3$^{-/-}$/6$^{-/-}$ mice. Data points represent mean ± SEM. Numbers represent the number of rings. Data from Ctr and *trpc*6$^{-/-}$ mice at 100 µM CCh were analyzed using Student´s t-test. ***, $p < 0.001$.